IMPACT OF THE CONTROLLER MODEL COMPLEXITY ON MODEL PREDICTIVE CONTROL PERFORMANCE FOR BUILDINGS

Damien Picard[a,*], Ján Drgoňa[b], Michal Kvasnica[b], Lieve Helsen[a,c]

[a]KU Leuven, Department of Mechanical Engineering, Leuven, Belgium
[b]Slovak University of Technology in Bratislava,
Radlinského 9, SK-812 37 Bratislava, Slovak Republic
[c]EnergyVille, Thor Park, Waterschei, Belgium
[*]damien.picard@kuleuven.be

Abstract

Model predictive control (MPC) for heating, ventilation and air conditioning (HVAC) in buildings requires accurate controller models of the building envelope and its HVAC systems. Controller models are typically obtained by means of black- or grey-box system identification or using a white-box modelling approach. However, the necessary level of model complexity used by each method in order to obtain good MPC performance remains a priori unknown and no systematic method or examples showing the optimal complexity is available. This paper systematically investigates the required controller model complexity necessary to obtain optimal control performance for a given building. First, a 6-room house is modeled in detail using building energy simulation software. The building model is then linearised to obtain a linear time invariant (LTI) state-space model (SSM) and the upper bound of the control performance is computed using an MPC with the SSM both as controller and as plant model. The accuracy of the SSM (containing more than 250 states) is then artificially decreased by reducing its number of states to different orders ranging from 4 to 100 using balanced truncation model order reduction technique. The performances of MPCs using these controller models are then compared with the upper bound for both a standard MPC formulation (S-MPC) and an offset-free formulation (OSF-MPC) and with the performance of a rule-based-controller (RBC). The procedure is repeated for the same house model with a higher level of insulation and for a lighter weight construction. This paper shows that the controller model should contain a minimum of states to model each zone separately, and that the walls and floors separating the zones should also have enough states to act as a low pass filter with correct cut-off frequency. The minimum number of states further increases with the building mass content. In the case of the investigated 6-room house, the thermal comfort achieved by MPC using a controller model with a minimum of 30 states instead of 20 states was improved with a factor 2 to 6 without significant increase of the energy use, showing that good MPC performances require controller models with a significantly higher number of states than the order used by most of the black- and grey-box system identification techniques. The minimum required number of states might be chosen lower when OSF-MPC is used instead of conventional MPC. However, OSF-MPC might significantly increase the energy use when poor controller models (high model mismatch) are used. Furthermore, if the controller model is an LTI model, this paper shows that the CPU time necessary to solve the MPC optimization problem becomes independent of the number of states of the controller model when a dense approach is used. The controller model can thus be as complex as necessary to produce accurate predictions without increasing the computation time of the optimization.

Keywords: building climate control, optimization, model predictive control, model order reduction, controller model

1. Introduction

The number of papers about Model Predictive Control (MPC) for building in several journals is increasing every year exceeding more than 100 new papers in the journal Energy and Buildings in 2015. Despite these intensive research efforts the commercialization of MPC is still in its early stages. This is partially due to the lack of direct comparison (i.e., for the same scenario) of different optimization algorithms, of different controller models and their prediction performance, of the simulation parameters such as sampling time, prediction horizon and of climate forecast, as pointed out in the review paper by Hilliard et al. [1]. The main difficulty remains, however, to obtain a good controller model of the whole building with a minimum of effort as it is the most time consuming part [2, 3, 4, 5]. Detailed building energy simulation softwares (BES) such as EnergyPlus [6], TRNSYS [7] or Modelica (`Buildings` [8], `IDEAS` [9]) allow accurate building modeling but generate models which are too complex to be used in efficient optimization algorithms [2, 3]. Low order linear models are usually preferred due to their computational tractability [10]. Therefore, simplified models need to be generated by means of grey-box [11, 3, 12, 13] or black-box system identification such as auto regressive [14], subspace [4] and artificial neural network methods [15] or by simplified white-box modeling [16, 17, 18, 19, 20, 21].

While black-box identification has the advantage that no prior knowledge of the system is required and that it can deal more efficiently with large sets of data, its prediction performance for longer time horizons (e.g., more than 12 h) is not sufficiently accurate [11]. Grey-box system identification is more suitable for long time horizons but the method becomes very costly for large multiple-input multiple-output (MIMO) systems. As shown by [12, 13, 22] a good choice of the structure of the grey-box

model, i.e., its order, its inputs and its states, is crucial for its performance but this choice is very case specific. Therefore authors involved in the opti-control project [16, 17, 23], and others [18, 19, 20, 21] opted for a linear white-box approach where the model is set up based on geometrical and on physical data of the building and simplified physical laws. The authors all showed that this simplified approach could mimic the results (typically expressed as operative temperatures) of the more complex models obtained with BES software within an error margin of $\pm$ 0.5-1 K. By applying model order reduction methods, the complexity of the obtained linear model can be further reduced [23, 21, 20, 24]. Both for the grey-box and for the white-box approach, the necessary level of model complexity in order to obtain a good MPC remains unknown and no systematic method to determine this optimal model complexity is available [5, 25].

Some studies have investigated the influence of the model order on the model off-line prediction performance [26]. At the building component level, Gouda et al. [24] applied a non-linear optimization technique to optimally reduced higher order building component models to second order models. Xu and Wang [27] also reduced their model complexity to a second order model by minimizing the error between the frequency response of a higher order model and their model. Fraisse et al. [28] concluded that a wall should be represented by a fourth order model. At the multi-zone building level, Sturzenegger et al. [23] and Kim and Braun [21] created a linear model with a large number of states and they reduced the order by applying Model Order Reduction (MOR). Foucquier et al. [20] also started from a high order building model but they reduced the complexity by merging different walls together. However, to the authors' best knowledge, no work has been presented yet which focuses on the investigation of the influence of the controller model accuracy on the performance of building climate controllers. The studies mentioned above only considered the off-line prediction errors without quantifying their impact on the controller performance.

The main contribution of this paper is the performance comparison of an MPC which uses the same controller model as the plant model such that no model mismatch is present, with MPCs using controller models of different orders. This paper is the first to systematically assess the performance of MPCs for a given building using controller models of different orders without relying on system identification but using linearization and model order reduction techniques instead. This means that each reduced order model is *the best possible linear representation* of the building with that given number of states as each remaining state is optimally chosen by the model order reduction technique. This study shows that the minimum number of states of the controller model necessary to obtain optimal control performance is higher than typical orders used in black- and grey-box methods. This is confirmed by Picard et al. [29] where a white-box MPC shows 50% more savings than a grey-box MPC for the same building. This paper further shows that the MPC computational time can become independent of the number of states of the controller model by using a dense formulation as long as the controller model is linear. The paper also investigates how its conclusions change when an off-set free MPC is used instead, and the dependency of the computational time on the controller model complexity.

For this purpose, a six rooms house is modeled in BES software which is then linearized and reduced to a set of linear, time invarient (LTI) reduced order models (ROM) using a model order reduction technique (see Section 3). Different types of building climate controllers (BCC) are developed (Section 4): a traditional rule-based-controller (RBC), MPC in standard form (S-MPC) and MPC using an off-set free approach (OSF-MPC). Section 4 further describes the controller objectives, the state observer and the quadratic cost function of the MPCs as well as the state condensing approach which is used to improve the computational tractability of the simulations. The tuning and the performance evaluation of the different controllers for a full year simulation are described in Section 5.

2. Methodology

This paper investigates the influence of the controller model accuracy on the evaluation of building climate controller performance and the minimum number of states necessary to obtain optimal control performance. The methodology is graphically represented in Fig. 1.

For this study, an existing small house is modeled using the open-source Modelica library `IDEAS` [9]: a state-of-the-art building energy simulation program. The existing building is used to ensure reasonable parameter values but no validation has been performed between the reference building model and the real building. While the Modelica reference building model is accurate in the physics it describes, its mathematical formulation combines non-linear partial differential equations, ordinary differential equations and algebraic equations. However, the non-linear model can be accurately linearized around a given working point (see Section 3.2), and as such it can be transformed into a form of linear time-invariant state space model (SSM) [18]. The obtained SSM can then be used for simulations or control purposes in a high-level mathematical environment such as MATLAB ®. In this paper, the obtained SSM will be used as plant model such that no model mismatch between controller model and plant model is present when the MPC uses the (not reduced) SSM as controller model. This case is the theoretical benchmark.

In order to artificially vary the complexity and accuracy of the controller models, the obtained SSM can be reduced to different orders (see Section 3.3). The model order reduction (MOR) will decrease the complexity of the model as well as its ability to predict the thermal behavior of the building. The obtained ROMs are used to mimic the best possible low order controller models which can be obtained for these orders by means of system identification, for example.

Finally, the influence of the controller model complexity is investigated by evaluating the thermal comfort, the energy use, the computational effort (CPU) and the prediction error of the different MPCs, each using a controller model with a different complexity while the building model is kept unchanged. Additionally, MPC performance is compared with a traditional thermostat

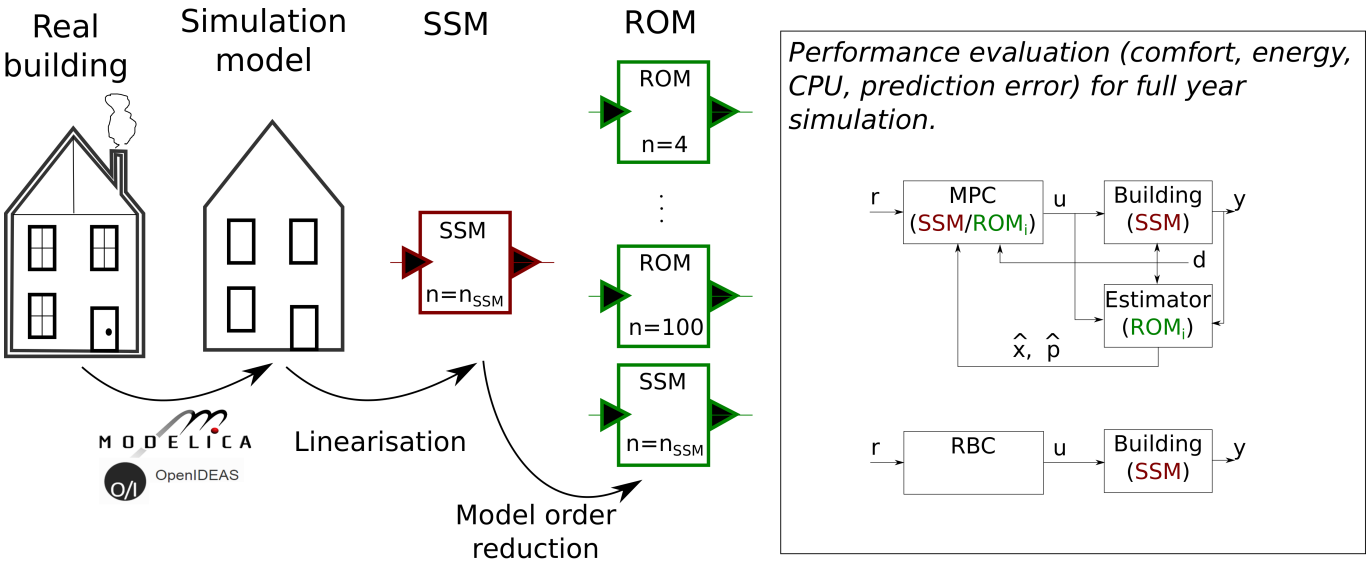

Figure 1: Schematic view of the methodology. From left to right: a 6-room house is modeled using the BES Modelica library `IDEAS`*. The obtained model is then linearized and converted to a time-invariant SSM. Balanced truncation MOR technique is used to obtain ROMs of different orders. Finally, the upper bound of the controller performance is computed by using the SSM model both as controller and plant model (theoretical benchmark). The performances of the MPC using the different ROMs as controller model are compared with the upper bound and with a RBC.*

Figure 2: Picture of the modeled house (Bruges, Belgium).

Table 1: General building parameters.

Floor area	[m^2]	56
Conditioned volume	[m^3]	130.6
Total exterior surface area	[m^2]	195
Window to wall ratio	[-]	19%
Windows orientation	[-]	North-East

RBC.

In order to generalize the results, the same methodology is repeated for three different scenarios (see Section 3.1): 1) the original building, 2) the same building but with an improved insulation level (renovated building), and 3) the same building but with light-weight wooden walls instead of concrete walls (lightweight building).

3. Building modeling

Building energy simulation (BES) programs are simulation tools that simulate the energy flows in buildings. This includes the interaction between the building envelope and its surroundings (i.e., weather, radiation heat losses, etc.), between the building envelope and its HVAC system and possibly between the HVAC system and the electrical grid. BES programs use physical equations to describe the systems.

This section describes the modeling of an existing house (Section 3.1) in the BES program `IDEAS` and its linearization in order to obtain a SSM (Section 3.2). Section 3.3 describes furthermore the applied model order reduction technique and Section 3.4 analyses the open-loop behavior, the frequency response and the prediction performance of the obtained ROMs.

3.1. Building and building model description

The plant model is based on an existing small 6-room terraced house in Bruges, Belgium (see Fig. 2) with general parameter values given by Table 1. The heating system is composed of one radiator per room fed by a central gas-boiler. The original building is badly insulated and it has a poor air-tightness. The column *Original* of Table 2 gives its overall heat transfer coefficient (U-value), its maximum volume air change per hour (ACH) and the composition of its outer walls, floors, windows and roof. For the renovated case, the U-value is decreased by adding insulation to the outer walls (see column *Renovated* in Table 2). The thickness of the insulation layer varies for the different outer walls, respecting the actual renovation plans of the building. Finally, the case of a light-weight building is considered by replacing all outer walls and the roofs by an insulated wooden structure which leads to a better insulation and a lower building mass. The last row of the table indicates the number of state variables of each model.

Table 2: Parameter values and number of states in the BES model for the original, the renovated and the light weight buildings.

		Original		Renovated		Light weight	
Av. U-value	[W/m^2/K]		1.28		0.65		0.36
ACH	[1/h]		8.7		4.1		4.1
Outer walls	[m]	Concrete	0.268	Concrete	0.200	Wood + insulation	0.150
	[m]	Plaster	0.010	Insulation	0.015-0.115		
				Plaster	0.010		
Floors	[m]	Reinforced concrete	0.120	Reinforced concrete	0.120	Reinforced concrete	0.120
	[m]	Screed	0.040	Insulation	0.020	Insulation	0.020
	[m]	Topping	0.060	Screed	0.060	Screed	0.060
	[m]	Tiles	0.030	Tiles	0.030	Tiles	0.030
Windows		Double glass (g=0.75, U=1.4 W/m^2/K)		Double glass (g=0.75, U=1.4 W/m^2/K)		Double glass (g=0.75, U=1.4 W/m^2/K)	
Roof	[m]	Fibre-cement	0.180	Fibre-cement	0.180	Wood + insulation	0.200
	[m]	Insulation	0.080	Insulation	0.080		
	[m]	Plaster	0.010	Plaster	0.010		
# States			283		286		250

In this study, only the building envelope, consisting of 6 thermal zones, 5 windows, 11 outer walls, 5 boundary walls with neighboring buildings, 6 roof surfaces, 3 floor surfaces on the ground, 3 floor surfaces between the ground floor and the first floor, and 6 internal walls between the zones, is considered. The heating system is idealized as a perfectly controllable, limited heating power which can directly be injected in each room. The radiators and the gas boiler are thus not modeled but they are replaced by one heat input per zone.
The building envelope is modeled using the Modelica `IDEAS` library [9]. `IDEAS` (Integrated District Energy Assessment by Simulation) is a recently developed district energy commodity flow modeling environment which enables multi-zone thermal building simulation, including building envelope, heating, ventilation and air-conditioning systems, and electric system simulation. The governing equations are discretised partial differential equations, ordinary differential equations and algebraic equations, which are solved simultaneously. For a complete description we refer to [18] and to [30].

3.2. Linearization of the IDEAS building thermal model

The Modelica building envelope model, as implemented using the `IDEAS` library, is not directly usable as controller model due to its high complexity. As explained in Section 2, the Modelica reference building model is linearized around a working point in order to obtain a linear SSM. Picard et al. (2015) [18] showed that for a typical Belgium weather ([31]) the linearization error for these equations remains typically below 1 K. However, the equations for the solar transmission and absorption through the windows are highly non-linear and they should not be linearized. The solar transmission and absorption are instead pre-computed using the `IDEAS` model and they are considered as inputs to the linearized SSM. For a complete description of the linearization process we refer [18].
The obtained SSM has the following form:

$$\frac{\partial x(t)}{\partial t} = A_c x(t) + B_c u(t) \tag{1a}$$

$$y(t) = C_c x(t) + D_c u(t) \tag{1b}$$

All states x represent temperatures. The input vector u contains the control variables, i.e., the heat flow from each radiator to its room (composed of 40% of radiative and 60% of convective heat flow), and the disturbances, i.e., the ambient temperature and the ground temperature, the heat absorbed by and the direct and diffuse solar radiation transmitted by each window, and, finally, the direct, diffuse solar radiation and the environment temperature (i.e. a radiation temperature taking both the environment and the sky temperature into account) per orientation and inclination present in the model. Fig. 3 gives the temperature error between the non-linear `IDEAS` models for the three building types and the obtained SSM. The errors are computed for a full year open-loop simulation, i.e. the SSMs are never re-initialized with the non-linear models. A standard weather file of Uccle, Belgium ([31]) is used to represent the weather condition and each zone temperature is kept within its comfort range using a PID-controller. All inputs of the non-linear and the linear models are exactly the same. As Fig. 3 shows, all outlier errors are below $\pm$1K and the median of the error is close to zero for each zone. This confirms that the obtained SSMs with pre-computed inputs are accurate approximations of the non-linear `IDEAS` models. The obtained SSMs will be further referenced as *building models*.

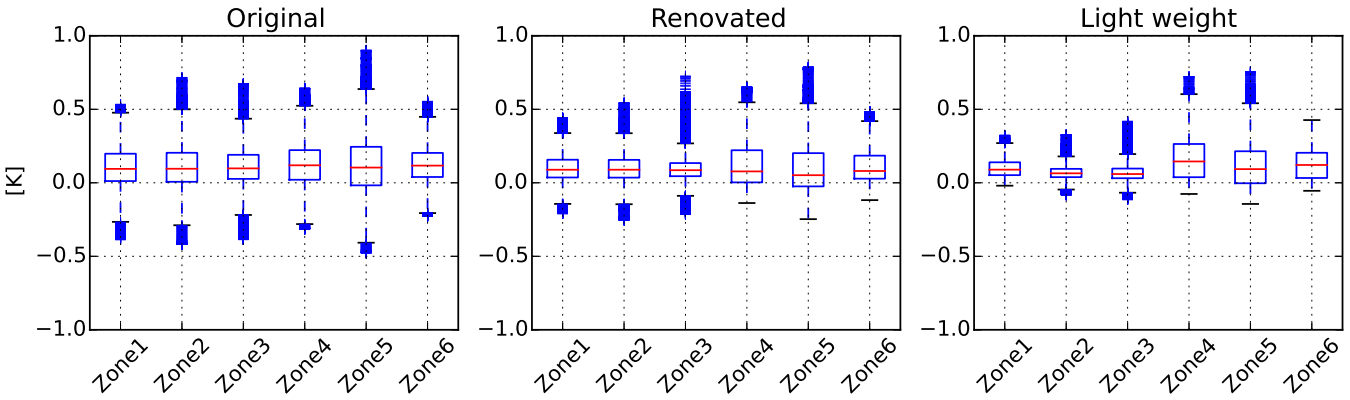

Figure 3: Boxplot of the temperature error between the non-linear `IDEAS` *models and their linear state space models for a full year open-loop simulation. The errors are given for each building type. The centered line gives the median, the box gives the first and third quartiles, the wiskers contain 99.5% of the data, and the crosses are the outliers.*

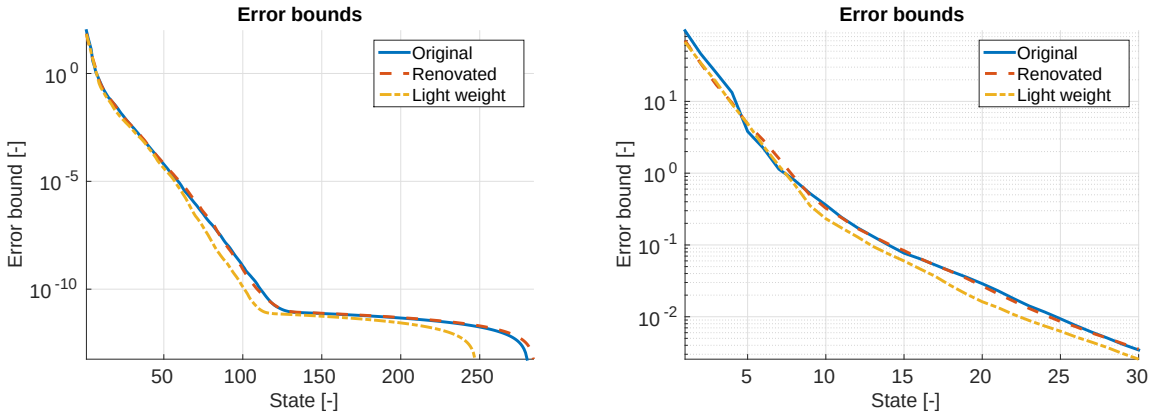

(a) Error bounds for all ROMs.

(b) Error bounds for ROMs with 30 highest energy states.

Figure 4: Error bounds of the ROMs generated from the original SSMs.

3.3. Model order reduction

Model order reduction (MOR) is an umbrella term for methods used for reducing the computational complexity of mathematical models. The method reduces the model associated state-space dimensions in order to reduce the computational cost of model evaluation. The reduced model is, however, less accurate.

3.3.1. Balanced Truncation

In this paper, the square root balanced truncation algorithm is used to obtain the ROMs of different orders. The command `reduce` of MATLAB with default settings is used. This method is based on the Hankel singular values (HSV) and was chosen because it guarantees an error bound and preserves most of the system characteristics in terms of stability, frequency, and time responses [32]. Furthermore the HSV of the building models decrease rapidly, the HSV based method gives accurate models even for very low-orders [33]. The error bound of the balanced truncation method is given by:

$$\sigma_m \leq ||M - \hat{M}||_\infty \leq 2 \sum_{i=m+1}^{n} \sigma_i. \tag{2}$$

with σ_i the HSVs of the original model, M and $\hat{M}$ the amplitude of the frequency response of the original and of the reduced models, $||M - \hat{M}||_\infty$ their infinity norm (i.e., the maximum difference between the two responses) and n and m the order of the original and of the reduced models [34]. Note that the HSV σ_i are sorted from large to small. For a complete description of the calculation of the HSV and of the balancing method we refer to [32] and [34].

Fig. 4 gives the error bound for the three building models for different reduction orders. As expected, due to the rapidly decreasing HSVs of the models, the error bounds decrease rapidly with the increase of the ROM order. Based on this graph, a set of ROMs with orders ranging from 4 to 100 is chosen to investigate the influence of the model complexity.

3.3.2. Reduced order model initialization and discretization

When applying MOR, the initial state values also need to be transformed in their reduced form. However, the MATLAB function `reduce` does not provide the transformation matrix. As the physical meaning of the initial states for the reduced models is lost by MOR, the initialization of reduced models is not straightforward. This section describes how the original SSM can be adapted to have zero initial state values without changing its input-output behavior.

We assume a LTI SSM in continuous time domain with a given initial states value $x_0 = 293.15$ K. Because x_0 is a constant the SSM (1) is equivalent to:

$$\frac{\partial\left(x(t) - x_0\right)}{\partial t} = A_c\left(x(t) - x_0\right) + B_c u(t) + A_c x_0 \tag{3a}$$

$$y(t) = C_c\left(x(t) - x_0\right) + D_c u(t) + C_c x_0 \tag{3b}$$

By substitution $\bar{x}(t) \coloneqq (x(t) - x_0)$, the model can be compactly rewritten as follows.

$$\frac{\partial \bar{x}(t)}{\partial t} = A_c \bar{x}(t) + \begin{bmatrix} B_c & A_c x_0 \end{bmatrix} \begin{bmatrix} u(t) \\ 1 \end{bmatrix} \tag{4a}$$

$$y(t) = C_c \bar{x}(t) + \begin{bmatrix} D_c & C_c x_0 \end{bmatrix} \begin{bmatrix} u(t) \\ 1 \end{bmatrix} \tag{4b}$$

The new SSM with state variables $\bar{x}$ has an initial states vector $\bar{x}_0 = 0$. The reduced model can now also be initialized at zero.

The discretization of the transformed continuous SSM (4) is necessary because the controller design and the simulations will be performed in discrete time domain. Based on the relevant dynamics and associated time constants, the unified sampling frequency $T_s = 15$ min was used as a motivated choice for all investigated model types. The discretized model has the following form

$$x_{k+1} = Ax_k + Bu_k + Ed_k + G, \tag{5a}$$

$$y_k = Cx_k + Du_k + H. \tag{5b}$$

where x_k, u_k and d_k are states, inputs and disturbances at the *k*th time step, respectively. The B_c matrix of the continuous SSM (4) contains both the control inputs u and the disturbances d. However, for control purposes it is necessary to separate them into individual matrices. The B_c matrix is therefore split into an input matrix and a disturbance matrix which correspond, after discretization, to the matrices B and E of Eq. 5. The constant value matrices G and H are necessary to include the initial conditions, as explained above.

3.4. Off-line analysis of the ROMs

This section compares the behavior of the original SSM with the different ROMs. The temperatures obtained by an open-loop simulation are compared, the prediction performance is computed for different horizons and the frequency response of each model is analyzed using bode-plots.

Fig. 5 shows the temperatures of each zone obtained by the SSM (dashed-line) and by the ROMs for the renovated building case. These profiles are obtained by a four days simulation with realistic control inputs (taken from a previous MPC simulation using the SSM as controller model) and disturbances. From Fig. 5, one can see that ROMs of order below 20 cannot describe the temperature of each zone accurately. The ROM of order 15 shows, for example, a good fit for all zones except for zones 1 and 2 with a maximum temperature error of 1 K. The fact that only some zone temperatures are predicted accurately by low order ROMs while other zones are not, illustrates that the zones are not strongly correlated with each other. Therefore, each zone needs to be modeled by a minimum set of states which describe their own dynamics, as their temperature cannot be expressed by a linear combination of the neighboring zone temperatures. While the thermal interaction between the zones is weak, Fig. 6 indicates that the interaction is not negligible for low frequency excitations. Fig. 6 presents the frequency response of the zone temperatures 1 and 2 as a function of the heat inputs to zones 1-6 for the SSM (solid black line) and the different ROMs for the renovated building case. The graph (1, 1) of Fig. 6 shows that zone 1 acts as a low pass filter on the heat injected in the same zone (Q(1)). The graphs (1, 2) to (1, 6) show that the temperature of zone 1 is also influenced by the heat inputs of the neighboring zones if the heat input frequencies are lower than 10^{-5} Hz (i.e., 1 day). Higher frequencies are damped out by the internal walls between the zones. The frequency responses of the ROMs, however, differ from the SSM. They are overestimating the influence of the heat inputs on the neighboring zones for high frequencies. This is due to the lack of states available to physically separate the zones from each others. The ROMs of order 4 and 10 show large errors even for low frequencies due to the inaccurate zones representation. The frequency responses to solar gains are similar as the heat is injected in a similar way to the zone as the controlled heat inputs. The frequency response to the ambient temperature is plotted in Fig. 7 for zones 5 and 6. From Fig. 7, one can see that the responses of all ROMs except the one of order 4 are accurate. This means that the building insulation is correctly modeled by all ROMs of order above 10.

Fig. 8 shows a boxplot of the 1, 10 and 40-step ahead prediction errors of all zones for the different ROMs for the original

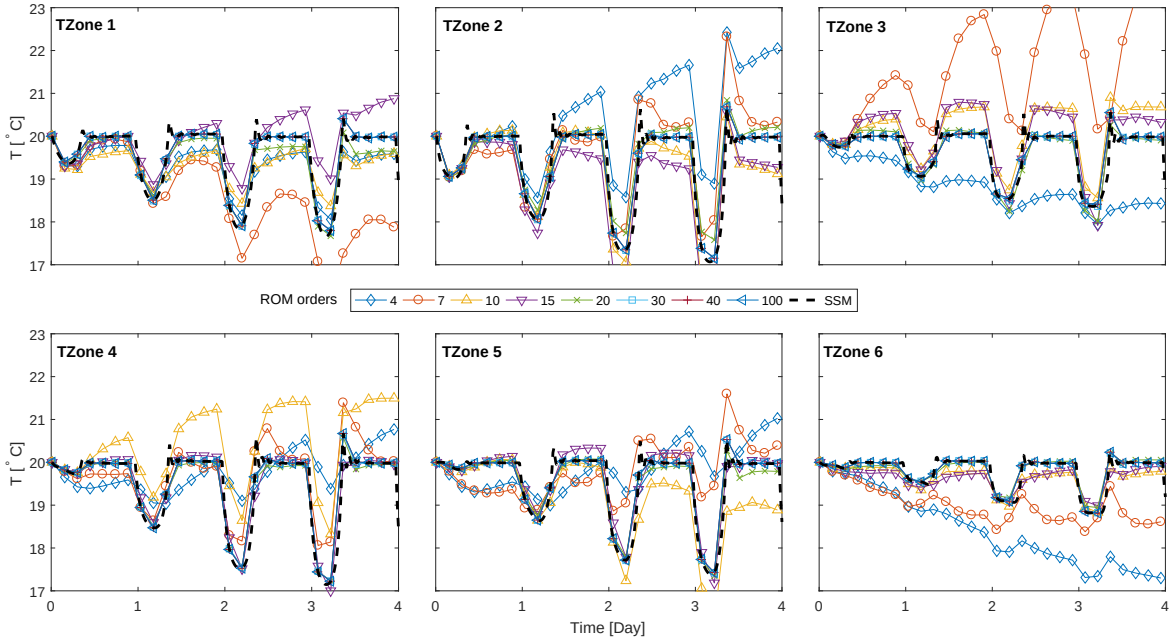

Figure 5: Zone temperatures for four days open-loop simulation. The same inputs are applied to the SSM (dashed-line) and to the ROMs (colored line).

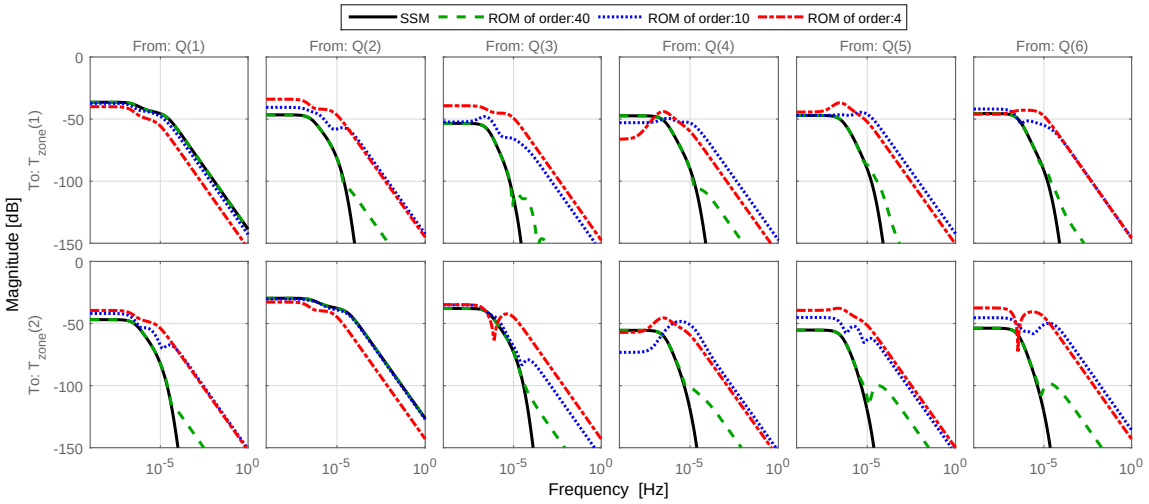

Figure 6: Frequency responses of zones 1 and 2 to the heat inputs of zones 1-6 for the renovated building.

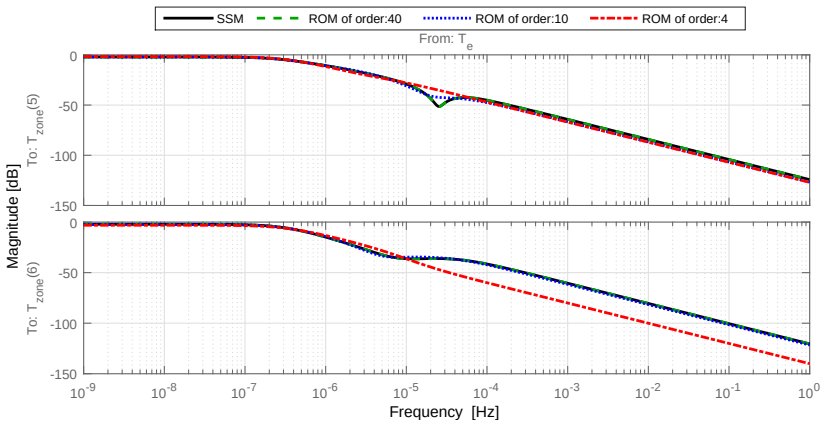

Figure 7: Frequency responses of zones 5 and 6 to the ambient temperature for the renovated building.

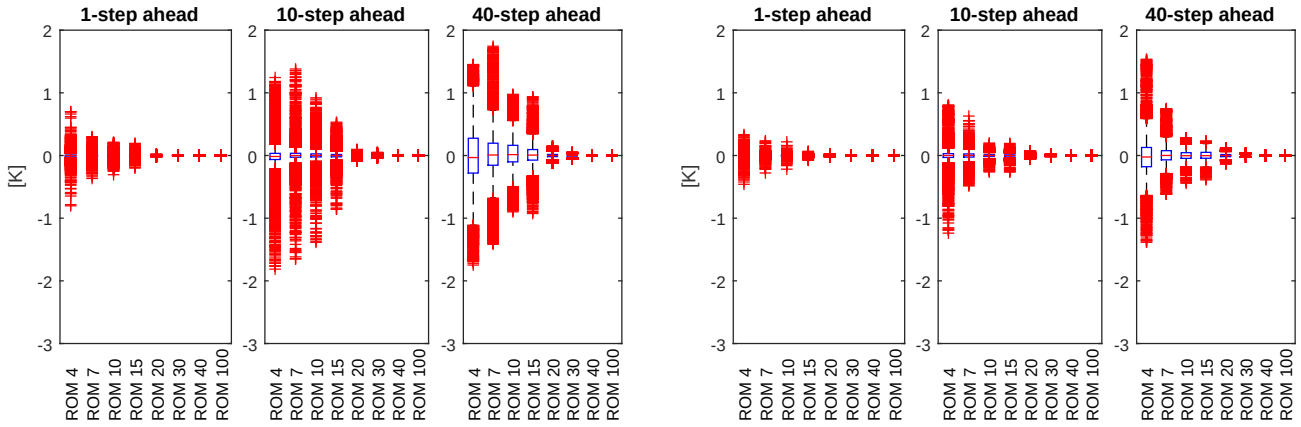

(a) Original *(b) Light weight*

Figure 8: Box-plot of the n-step ahead prediction error of all zone temperatures for different ROMs for the original building (left) and the light weight building (right). The centered line gives the median, the box gives the first and third quartiles, the whiskers contain 99.5% of the data, and the crosses are the outliers

building (Fig. 8a) and the light weight building (Fig. 8b). The N-step ahead prediction error at time k (ϵ_k^N) is defined as the difference between the SSM outputs and the ROM outputs at time $k+N$ when the same inputs $u = [u_k, \cdots, u_{k+N}]$, disturbances $d = [d_k, \cdots, d_{k+N}]$ and equivalent initial state values x_k and $\tilde{x}_k$ are fed to the models:

$$\epsilon_k^N = F(x_k, u, d) - f_i(\tilde{x}_k, u, d) \tag{6}$$

with F and f the transfer function of the SSM and the ROM, respectively.
The errors for the renovated building scenario are not given as they are very similar to the original building. Comparing Fig. 8a with Fig. 8b shows that ROMs of the same order have a lower prediction error for the light weight building than for the heavier original building. This is due to the higher mass content of the heavy building which requires a finer discretization of this mass to model the heat diffusion accurately. Remarkably, while Fig. 5 shows that the error per zone is high for the ROMs of order below 20, all medians of Fig. 8 are very close to zero. This means that the average building temperature (i.e., the average of all zone temperatures) is still correct for all ROMs.

4. BUILDING CLIMATE CONTROL

Building climate controllers are responsible for the comfort experienced in buildings. The controller controls the HVAC of the building ensuring that comfort (i.e., temperature, CO_2 concentration, etc.) remains in each room in its prescribed time-dependent range. As a similar comfort can be achieved with different sequences of control actions, the required energy to maintain the building in its comfort bound can vary significantly with the controller algorithm type.
In this section, we focus on thermal comfort, whereby the thermal comfort and the energy use objectives are firstly defined (see Section 4.1). Section 4.2 introduces a traditional rule-based-controller (RBC). Finally, Section 4.3 discusses the different implementations of a model predictive controller (MPC) considered in this paper. The meaning of the symbols used to describe the variables and the parameters of the different controllers, together with their values are listed in Table 3 and Table 4, respectively.

Table 3: Notation of variables used in Section 4.

Notation	Units	Description	Control setup
x	$[K, -]$	Temperatures for the SSM, No physical meaning for the ROM	States
y	$[K]$	Room temperatures	Outputs
r	$[K]$	Desired room temperatures	References
u	$[W]$	Radiators heat flows	Inputs
d	$[K, W]$	Temperatures, heat flows and radiation gains	Measured external disturbances
p	[-]	Augmented state variables	Unmeasured internal disturbances
s	$[K]$	Comfort violations	Slack variables

Table 4: Notation of parameters used in Section 4.

Notation	Units	Description	Values
ub	$[K]$	Upper comfort boundary	$[297.15, 299.15]$
lb	$[K]$	Lower comfort boundary	$[293.15, 296.15]$
N	[-]	Prediction horizon	40
Q_{s}	[-]	Comfort weighting matrix	1×10^8
Q_{u}	[-]	Heating weighting matrix	1
n_x	[-]	Number of states	see Fig. 1
n_u	[-]	Number of inputs	6
n_y	[-]	Number of outputs	6
n_p	[-]	Number of augmented states	6
n_d	[-]	Number of measured disturbances	44

4.1. Control objectives

A building automation and control system (BACS) governs buildings such that certain comfort and economic criteria are fulfilled. Instead of tracking particular reference values, a BACS typically considers comfort ranges. The task is then to manipulate the building inputs such that required comfort criteria are kept within the range while the total amount of used energy is minimized. It should be noted that the comfort and the energetic criteria are often competing as the increase of comfort typically leads to an increase of energy use. In this paper, thermal comfort is the most emphasized objective, treated as soft constraint to guarantee a solution.

4.1.1. Thermal comfort

The thermal comfort objective is achieved by maintaining each room temperature y_i of the house in the comfort range as defined by the European standard ISO-7730. The lower and upper temperature bounds (lb, ub) vary between $[20, 23]^\circ C$ and $[24, 26]^\circ C$, respectively, as a function of the 7-days average of the ambient temperature. The comfort objective corresponds thus to the constraint:

$$lb_k - s_k \leq y_{i,k} \leq ub_k + s_k \tag{7}$$

with s the relaxation variable which should be minimized and the index k the sampling time.

4.1.2. Minimization of energy use

The second objective is to use a minimal amount of energy to achieve the comfort. In this paper, the energy use is the sum of the thermal energy injected by all radiators. The RBC was tuned such that it keeps the zone temperatures as close as possible to the lower comfort bound, but without endangering the comfort. For the case of MPC, both the energy use and its derivative are minimized such that power peaks are avoided.

4.2. Standard building control strategies

Usually the controller consists of a set of rules which determine the control action as a function of inputs (e.g., a room temperature, the outside weather conditions, etc.) and a set of set points. These types of controllers are the so-called rule-based controllers (RBC). They are widely used for residential buildings because of their simple design and configuration and their low computational demands allowing cheap hardware solutions. Their main drawbacks are that they are not adaptive, not flexible, not predictive and they need to be tuned. RBCs cannot track a time-varying reference or minimize the energy necessary to stay within a bound. The RBC implementation used in this paper is described in Section 4.2.1.

4.2.1. Rule based controller (RBC)

The commonly used controller for residential buildings with central heat production and radiators is a hysteresis rule based controller (RBC) also called central thermostat controller. Its working principle is as follows: a temperature sensor is placed in the main room, typically the living room. Based on this temperature and a comfort range, the central heating is turned on or off. Hot water can only flow to the radiators when the central heating is on. All radiators are equipped with thermostatic valves, except those in the room of the thermostat. The valve acts as a proportional controller by controlling the water mass flow rate through the radiator and so controlling its power.
The supply temperature T_{sup} is for all radiators the same and it is calculated using a typical heat curve equation:

$$T_{sup} = r + \left(\frac{T_{sup,n} + T_{ret,n}}{2} - y_{j,n} \right) q^{1/m} + \frac{T_{sup,n} - T_{ret,n}}{2} q \tag{8}$$

$$q = \frac{r - (T_{e,6h} + \epsilon)}{y_{j,n} - (T_{e,n} + \epsilon)} \tag{9}$$

where *sup* and *ret* stand for supply and return water temperatures, the subscript *n* refers to the nominal conditions ($T_{sup,n} = 70°C$, $T_{ret,n} = 50°C$, $T_{e,n} = -10°C$), and the index *j* refers to the room with the thermostat. The exponent *m* depends on the heating system (for radiator, $m = 1.3$). A correction term $\epsilon = 8$ K on the outside temperature $T_{e,6h}$ (averaged over 6 h) is added to take the solar gain into account.
The binary control action z_k of the central heating in *k*th time step, based on the temperature measurement in *j*th (central) room $y_{j,k}$ and given reference temperature r_k is defined by a switching rule of the relay based thermostat given by following equation

$$z_k = \begin{cases} 1 & \text{if} \quad (z_{k-1} = 1 \ \wedge \ (y_{j,k} \leq r_k + \gamma)) \vee \\ & \qquad (z_{k-1} = 0 \ \wedge \ (y_{j,k} \leq r_k - \gamma)) \\ 0 & \text{otherwise} \end{cases} \tag{10}$$

where $\wedge$ is the logic conjunction and $\vee$ denotes for the logic disjunction. The parameter 2γ here represents the width of the hysteresis. The values of the control action represent the heating mode if $z_k = 1$ and not heating if $z_k = 0$.
Finally the actual power $u_{i,k}$ delivered by the *i*th radiator to the *i*th zone at the *k*th time step is given by:

$$u_{i,k} = \begin{cases} G_i z_k (T_{sup,k} - y_{i,k}), & \text{if } i = j \\ \alpha_i G_i z_k (T_{sup,k} - y_{i,k}), & \text{otherwise} \end{cases} \tag{11}$$

with $\alpha_i \in [0, 1]$ the proportional gain of the thermostatic valve and G_i the total thermal conductance of the radiator. Each radiator is sized such that its maximum power is required when the outside temperature drops to $-10°$C. The same power bounds are used for MPC.

4.3. Model predictive building control

Model predictive control (MPC) is a control strategy which optimizes the control actions over a finite time-horizon by anticipating the effect of these actions, of the future disturbances and of the future constraints on the system. The ability of anticipation comes from the mathematical model of the system (i.e., the *controller model*) and the prediction of the future disturbances. Moreover MPC has the ability to directly take into account given control objectives (see Section 4.1), by penalizing them in the cost function of the optimization problem. The main drawback of this strategy is the difficulty of obtaining an accurate and computationally efficient controller model and the high computational cost (CPU) needed to solve the optimization problem.
The following sections describe the general controller setup (Section 4.3.1), the state estimator (Section 4.3.2) and the MPC objective function and constraints (Section 4.3.3). Section 4.3.4 describes the *state condensing method* which is used to speed up the algorithm.

4.3.1. Model predictive control setup

Fig. 9 illustrates the MPC setup used in this paper. The control loop consists of the building model representing the real building, the estimator, and the MPC which is composed of a controller model, an objective function and a set of constraints. In this paper, the building is simulated using the SSMs obtained by the linearization of the Modelica models (see Section 3). Two cases are considered: a standard MPC (S-MPC) and an off-set free MPC (OSF-MPC). In the case of S-MPC, the estimator is used to estimate the state values $\hat{x}$ of the controller model. In the case of OSF-MPC, a set of extra states p is added to the controller model to take into account the mismatch between the controller model and the building model. In that case the estimator also estimates $\hat{p}$ (see Section 4.3.2). We assume that the building is affected by disturbances d (e.g., weather conditions), which are measured and used as perfect predictions (with zero prediction error) by MPC and the estimator. MPC optimally manipulates the control action u, which represents the heat flow injected in the building. The feedback vector y consists of temperatures.

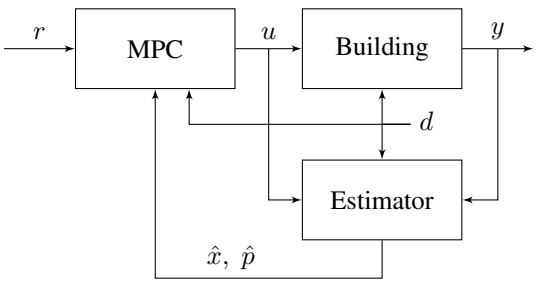

Figure 9: Schematic representation of the closed-loop system. Here, d are measured disturbances, y denotes the outputs, r are the output references, u are the control actions, and $\hat{x}$, $\hat{p}$ denote the estimates of the buildings states and building model mismatch, respectively.

4.3.2. State and disturbance estimation

A state observer is an algorithm that computes an estimate of the state values of the controller model based on the measurements of the inputs and outputs of the building model. In this paper, a standard Luenberger observer is used under the following form:

$$\hat{x}_{k|k} = \hat{x}_{k|k-1} + L\left(y_{m,k} - \hat{y}_{k|k-1}\right) \tag{12a}$$
$$\hat{x}_{k+1|k} = A\hat{x}_{k|k} + Bu_{k|k} + Ed_{k|k} \tag{12b}$$
$$\hat{y}_{k|k} = C\hat{x}_{k|k} + Du_{k|k} \tag{12c}$$

where the estimator gain L given as discrete stationary Kalman filter, was computed by the discrete Riccati equation using the `dlqe` MATLAB function. The subscript $k|k-1$ means that the value is estimated for time k based on the observed value of time $k-1$. The vector y_{m} denotes the vector of the measured outputs and the vectors $\hat{x}_k$ and $\hat{y}_k$ stand for the estimated states and outputs of the controller model, respectively.

Remark 1. *The matrices G and H due to the initialization transformation (see Section 3.3.2) are further omitted for the clarity of the notations. However, they are still included in the calculations.*

In the case of OSF-MPC, a set of extra fictitious states p, representing unmeasured internal disturbances, is added to the controller model to take the building model mismatch into account [35]. One extra state with a constant dynamic is added per each output of the controller model [36]. This approach, also called the active disturbance rejection control, allows us to consider a simpler controller model, since the modeling error is compensated in real time. The augmented controller model is now given by:

$$\underbrace{\begin{bmatrix}\hat{x}_{k+1}\\ \hat{p}_{k+1}\end{bmatrix}}_{\tilde{x}_{k+1}} = \underbrace{\begin{bmatrix}A & \mathbf{0}\\ \mathbf{0} & I\end{bmatrix}}_{\tilde{A}}\underbrace{\begin{bmatrix}\hat{x}_k\\ \hat{p}_k\end{bmatrix}}_{\tilde{x}_k} + \underbrace{\begin{bmatrix}B\\ \mathbf{0}\end{bmatrix}}_{\tilde{B}}u_k + \underbrace{\begin{bmatrix}E\\ \mathbf{0}\end{bmatrix}}_{\tilde{E}}d_k, \tag{13a}$$
$$\hat{y}_k = \underbrace{\begin{bmatrix}C & F\end{bmatrix}}_{\tilde{C}}\begin{bmatrix}\hat{x}_k\\ \hat{p}_k\end{bmatrix} + \underbrace{\begin{bmatrix}D\\ \mathbf{0}\end{bmatrix}}_{\tilde{D}}u_k. \tag{13b}$$

where the output disturbance matrix F was chosen as a full column rank identity matrix and all other matrices are the same as in Eq. 5.

Remark 2. *For the clarity of the notation, only the S-MPC equations will be used further. The equations for the case of OSF-MPC are obtained by replacing the matrices (A, B, C, D) by their augmented equivalent* $(\tilde{A}, \tilde{B}, \tilde{C}, \tilde{D})$. *For the observer, the gain* L *is also recomputed using the augmented matrices.*

4.3.3. MPC problem formulations

The aim of this section is to devise an optimal controller policy which minimizes the energy used while maximizing the thermal comfort for the occupants. The MPC optimization problem used in this paper is formulated in a quadratic way as follows

$$\min_{u_0,\ldots,u_{N-1}} \sum_{k=0}^{N-1} \left(||s_k||^2_{Q_\mathrm{s}} + ||\Delta u_k||^2_{Q_\mathrm{du}} + Q_\mathrm{u}u_k\right) \tag{14a}$$
$$\text{s.t. } x_{k+1} = Ax_k + Bu_k + Ed_k, \tag{14b}$$
$$y_k = Cx_k + Du_k, \tag{14c}$$
$$lb_k - s_k \leq y_k \leq ub_k + s_k, \tag{14d}$$
$$\Delta u_k = u_k - u_{k-1}, \tag{14e}$$
$$\underline{u} \leq u_k \leq \overline{u}, \tag{14f}$$
$$x_0 = \hat{x}(t), \tag{14g}$$
$$\forall k \in \{0,\ldots,N-1\}. \tag{14h}$$

where x_k, u_k and d_k represent the values of states, the inputs and the disturbances, respectively, predicted at the *k*th step of the prediction horizon N. The predictions are obtained from the LTI prediction model given by Eqs (14b) and(14c). The lb_k and ub_k parameters represent the comfort range given by the constraints (14d), where the variables s_k are used as the indicators of a comfort violation. The min/max constraints for the control input amplitude are given by (14f). Equation 14e defines the difference of the control action and it is used to limit peak powers. Note that for $k = 0$, (14e) becomes $\Delta u_0 = u_0 - u_{-1}$ where u_{-1} is the control input applied in the previous sampling instant. The initial conditions of the problem (14g) are given as the

state estimates from the estimator, desired comfort boundaries, predicted disturbances and previous control input. For particular initial conditions, the optimization computes the sequence $u_0^*, \ldots, u_{N-1}^*$ of control inputs that are optimal with respect to the quadratic objective function (14a) and the constraints. The term $\|a\|_Q^2$ in the objective function represents the weighted squared 2-norm, i.e., $a^T Q a$, with the weighting matrices Q_{s}, Q_{u}, and Q_{du} given as positive definite diagonal matrices. The first term of the cost function minimizes the square of the comfort violations, the second term minimizes the fluctuations of the control input while the third term minimizes the energy used. The problem is defined in discrete time, for all time indexes k acquiring integer values (14h).

4.3.4. State condensing

In the problem formulation (14), each input and each state is considered as an optimization variable. However, the computation cost to solve a linear-quadratic control problem is $\mathcal{O}\left(N^3(n_x+n_u)^3\right)$, with N the control horizon, n_x the number of states and n_u the number of inputs [37]. If the solver makes use of the sparsity of the problem, the complexity of the problem becomes $\mathcal{O}\left(N(n_x+n_u)^3\right)$. Another approach is to use the so-called *state condensing* method which rewrites the large and sparse system into a smaller but denser form. In this method only the inputs are considered as optimization variable and the complexity becomes $\mathcal{O}\left(N^3 n_u^3\right)$. Due to the large number of states and relatively small horizon, the condensing method is the most appropriate method for this study.
The states can be eliminated by straightforward linear algebra substitutions as follows:

$$x_1 = Ax_0 + Bu_0 + Ed_0 \tag{15a}$$
$$x_2 = A\left(Ax_0 + Bu_0 + Ed_0\right) + Bu_1 + Ed_1 \tag{15b}$$
$$\vdots$$
$$\begin{aligned} x_{k+1} = {} & A^{k+1}x_0 + \ldots \\ & \left[A^k B \ldots AB\ B\right]\left[u_0^T \ldots u_k^T\right]^T + \ldots \\ & \left[A^k E \ldots AE\ E\right]\left[d_0^T \ldots d_k^T\right]^T \end{aligned} \tag{15c}$$
$$\begin{aligned} y_k = {} & CA^k x_0 + \ldots \\ & C\left[A^{k-1}B \ldots AB\ B\right]\left[u_0^T \ldots u_{k-1}^T\right]^T + \ldots \\ & C\left[A^{k-1}E \ldots AE\ E\right]\left[d_0^T \ldots d_{k-1}^T\right]^T + Du_k + Fp_0 \end{aligned} \tag{15d}$$

The state variables from the previous time instants are substituted into the subsequent state prediction equations. Recursively adopting this procedure we obtain an explicit formula (15c) for calculating the state update in the $(k+1)$th time step based only on the initial state condition and predicted control actions. The output equation (15d) with condensed states can now replace the Eqs. (14b) and (14c) of the controller model in the original MPC problem formulation (14).

5. Simulation case study

In this section we present the simulation results for the set of MPCs with varying complexity of the controller model as described in Section 2 and for the RBCs. Furthermore, three types of 6-zone buildings with different insulation level and thermal mass (see Section 3) are investigated in order to generalize the results. Finally, the effects of the off-set free approach and of the dense formulation are also investigated.
Section 5.1.1 describes the performance criteria used to evaluated the controllers' performance. The simulation parameters and the controller tuning are presented in Section 5.1.2 and 5.1.3 and Section 5.2 discusses the results.

5.1. Simulation setup

This section discusses the performance criteria, setup of the simulation parameters and tuning of the individual controllers. All parameters are chosen based on the explicit analyzes.

5.1.1. Performance criteria

The controller performances are evaluated using four performance keys: energy use, thermal discomfort, 1-step ahead prediction error and CPU time. The energy use corresponds to the heat delivered by the radiators and is expressed in kWh. The thermal discomfort is evaluated as the number of Kelvin hour that the operative zone temperatures are outside the comfort range, i.e. the sum of each violation computed as its magnitude times its duration. The discomfort is further divided by the number of zones to be comparable to any building. The 1-step ahead prediction error is the error between the prediction of the zone temperatures made by the Luenberger observer and the outputs of the building model at the next time step. Finally, the CPU time corresponds to the overall simulation time.

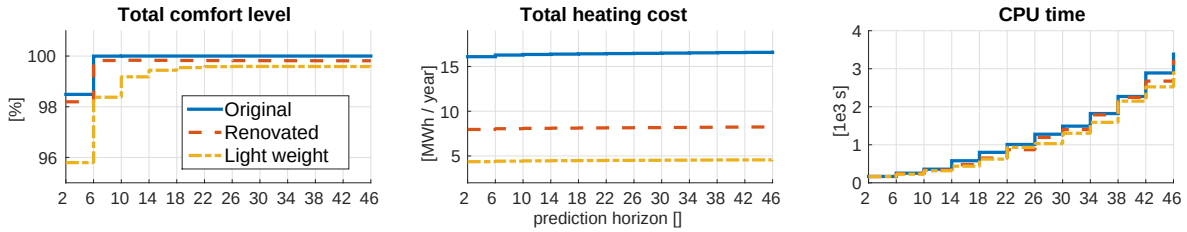

(a) Effect of the prediction horizon N.

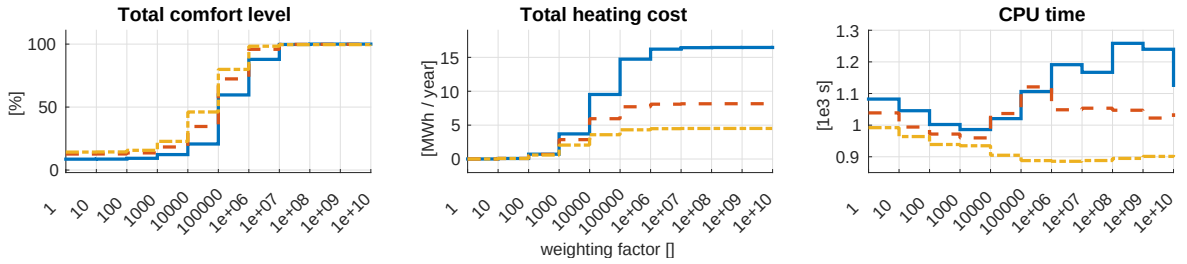

(b) Effect of the weighting factor $Q_s Q_u$.

Figure 10: Analysis of the MPC performance based on the change of the parameters N and $\frac{Q_s}{Q_u}$, while fixing the rest of the parameters.

5.1.2. Simulation parameters

Based on the dynamic response of the building models, the sampling period was chosen equal to $T_s = 900$ s. The maximum heating power of the radiators for each building, representing the upper bound on the control action, is shown in Table 5. The values are chosen such that the maximum powers correspond to the loads needed to achieve thermal comfort on the coldest days.

Table 5: Maximum heating power of the radiators (per zone).

Model type	Maximum radiator gains $\overline{u}$ $[W]$
Original	$[2940\ 960\ 300\ 1400\ 460\ 253]^T$
Renovated	$[1680\ 685\ 154\ 1000\ 320\ 232]^T$
Light Weight	$[840\ \ 343\ \ 77\ \ 500\ \ 160\ 116]^T$

The state values $x(0)$ are initialized to $20°C$, based on the procedure described in Section 3.3.2. The disturbance vector d was generated from a typical year in Uccle, Belgium [31]. The overall simulation period was chosen to be a single year.

5.1.3. Controllers tuning

In order to improve thermal comfort satisfaction of RBC and as such ensuring a fair comparison with MPC, the reference temperature r_k is shifted slightly above the lower boundary of the comfort range lb_k. The reference is now given as: $r_k = lb_k + 2.5°C$, while the width of the switching zone is equal to $0.5°C$. As shown by Fig. 12, this shift was necessary to avoid too many comfort violations.

In case of MPC, the values of the prediction horizon N and the weighting factor Q_s/Q_u are chosen based on the dependence of the MPC performance on the parameter values, as shown in Fig. 10. With emphasis on thermal comfort satisfaction the choice of the prediction horizon is set to $N = 40$ steps (i.e., 10 hours), and weighting factor $Q_s Q_u = 10^8$. We assume here that MPC has full disturbances preview, hence the perfect weather predictions are provided. The comfort range is given by two time-varying parameters, lb_k and ub_k, representing the lower and upper bound, respectively as defined in Section 4.1 based on ISO-7730.

To demonstrate the behavior and to verify the tuning of the investigated controllers we provide the control profiles over a representative time window of 7 winter days. The corresponding disturbance profiles are given by Fig. 11. For the brevity we choose only the second zone of the original building as the behavior of the other zones and buildings is similar. The RBC profiles with characteristic switching behavior of the control action and oscillatory indoor temperature profiles are shown in Fig. 12. The high comfort satisfaction was achieved thanks to the conservative reference setting. The MPC profiles with full controller model complexity are presented in Fig. 13. Here we can observe the optimal behavior of MPC minimizing the consumed energy by keeping the zone temperature as close as possible to the lower comfort boundary.

The MPC is constructed in the MATLAB environment, using the modeling and optimization toolbox YALMIP [38]. The closed-loop simulation was performed by applying the optimal control inputs $u^\star(t)$, computed at each sampling instant T_s by MPC to the building model. The objective function (Eq. (14a)) is quadratic and all constraints are linear, therefore the problem (14) can be solved as a strictly convex quadratic program (QP). Such problems can be efficiently solved even for larger values of the

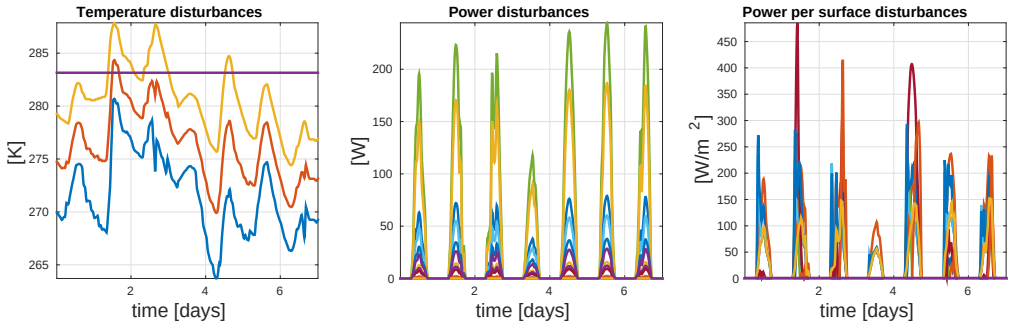

Figure 11: 7 days disturbance profiles. Left: temperature disturbances (ambient temperature (yellow), ground temperature (purple) and radiation temperatures). Middle: solar radiation through and absorbed by each window. Right: solar radiation per surface orientation. (For the interpretation of the references to color in text, the reader is referred to the web version of the article.)

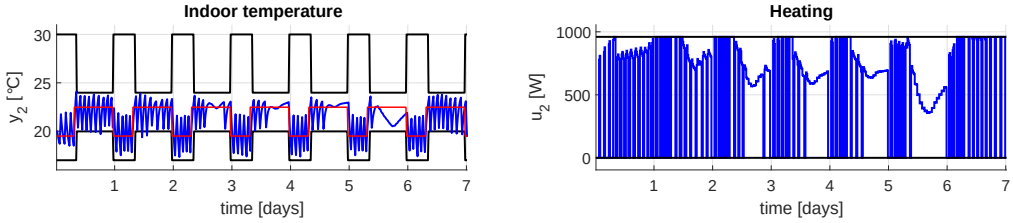

Figure 12: 7 days RBC profiles for the original building model. Left figure: closed-loop response of the indoor temperature (blue) in the second building zone w.r.t. the reference (red) and the comfort constraints (black). Right figure: corresponding profile of the control action (blue) w.r.t. the control boundaries (black). (For the interpretation of the references to color in text, the reader is referred to the web version of the article.)

prediction horizon, hence exploiting the full potential of the predictive control. In this study the state of the art optimization solver GUROBI [39] was used.

5.2. Results

Fig. 14 presents the performance key values for the full year simulations and for the three building types using different controllers. The bars represent the RBC and the MPCs with different ROMs as controller models. The stars represent the results for the equivalent OSF-MPCs. Fig. 14a shows that the comfort of MPC using the SSM as controller model is excellent with less than 30 Kelvin hour per year per zone (Kh/y/z) of discomfort for all buildings. The minimal comfort violations here are caused by the small overheating of the well insulated buildings during the hot days. This confirms that the radiators are sized properly and that the prediction horizon is long enough. The RBCs are also well tuned as they show a discomfort smaller than 300 Kh/y/z. The high comfort satisfaction achieved by RBCs, however, is coupled to additional energy use of 13, 15, and 12% compared to the highest order MPCs for the original, renovated and light weight building, respectively (see Fig. 14b).

Fig. 8 shows a decrease of the one-step ahead prediction error with an increase of the controller model complexity. Here the ROMs with $n_x \geq 20$ have negligible prediction error for all three building types. From Fig. 14 it appears that MPCs using a ROM of order lower than 30 score significantly worse than MPCs using a higher order ROM. This is due to the prediction error made by the observer, as shown in Fig. 14c. Fig. 8 showed that even with perfect initialization, the ROMs of order lower than 30 have non-negligible prediction errors. Fig. 14 confirms that the prediction errors directly influence the MPC results as the optimal controller is typically working near the comfort bounds. Even the very small error difference of 0.2-0.3K on the 40-steps ahead prediction between ROM 20 and ROM 30 (see Fig. 8) results in a significant difference in thermal discomfort with a factor between 2 and 6 for the number of Kh/y/z between the two MPCs. Good controller models are thus effectively crucial for multizone control. Note that obtaining an accurate 30 states controller model for a 6-zone building using SI is a challenging task [11].

Fig. 14a shows that OSF-MPCs using low order ROM achieve a significantly better comfort than S-MPC with the same model complexity. This comfort improvement, however, comes with an increase in the energy use (Fig. 14b) for the OSF-MPCs using very low order ROMs ($n_x \leq 15$). For ROMs with $n_x > 15$, the comfort improvement comes with a small or negligible increase in energy use. This can be explained by the prediction errors shown in Fig. 14c. The OSF approach adds one constant dynamic variable per output to the controller model, compensating the initialization error at each sampling instant, rather than improving the dynamical behavior of the ROM on the whole prediction horizon. Therefore when the model mismatch between controller model and building model is too large, the OSF method will not guarantee a good performance. By correcting the initialization value at each time step, oscillations may appear on the controller inputs. Overall, in the case of a sufficiently small model

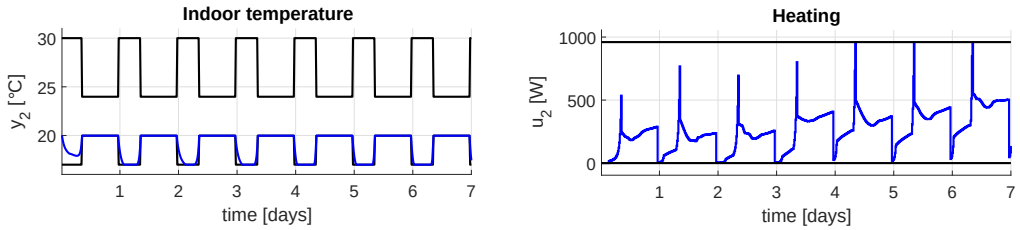

Figure 13: 7 days MPC profiles for Original building model. Left figure: closed-loop response of the indoor temperature (blue) in the second building zone w.r.t. the comfort constraints (black). Right figure: corresponding profile of the control action (blue) w.r.t. the control boundaries (black). (For the interpretation of the references to color in text, the reader is referred to the web version of the article.)

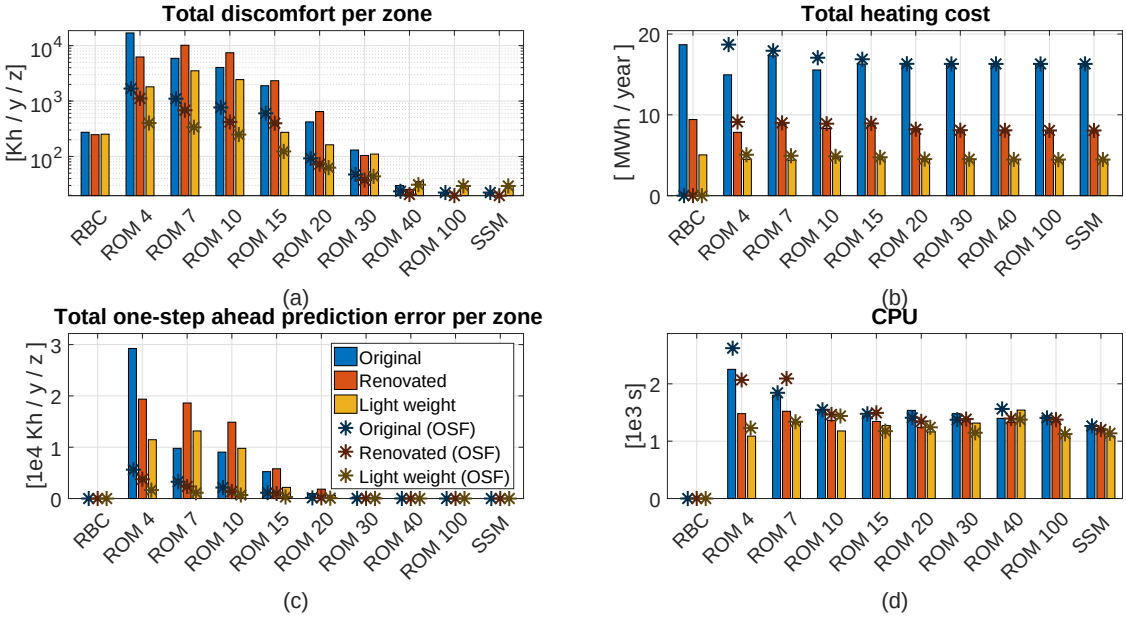

Figure 14: Comparison of performance keys evaluated for the RBC, S-MPC and the OSF-MPC approach for different controller model orders.

mismatch, the OSF method will improve the MPC results.

Finally, a reason to limit the controller model complexity is the computational effort required to solve the optimization problem. Fig. 15 shows, however, that when applying the dense approach as explained in Section 4.3.4, the CPU time becomes independent of the number of states. The CPU times for full year simulation scenarios and all building types using the dense approach have an average of 23.8 min with the maximum equal to 43.7 min and the minimum equal to 18.1 min with all computations performed on a 2.8 GHz machine with 2 CPU units each with 6 cores, under a GNU/Linux 64-bit Debian 3.16.7 operating system. As shown by Fig. 15 the sparse approach leads to intractable CPU times for a large number of states.

6. Conclusions

This paper systematically investigates the required controller model complexity necessary to obtained optimal control performance for a given building.

This paper shows that the controller model should contain a minimum of states to model each zone separately, and that the walls and floors separating the zones should also have enough states to act as a low pass filter with correct cut-off frequency. The minimum number of states further increases with the building mass content. In the case of the investigated 6-room house, the thermal comfort achieved by MPC using a controller model with a minimum of 30 states instead of 20 states was improved with a factor 2 to 6 without significant increase of the energy use, showing that good MPC performances require controller models with a significantly higher number of states than the order used by most of the black- and grey-box system identification techniques. The minimum required number of states might be chosen lower when offset-free MPC (OSF-MPC) is used instead of conventional MPC. However, OSF-MPC might significantly increase the energy use when poor controller models (high model mismatch) are used. Finally, the paper shows that the computational effort required to solve the optimization problem becomes independent on the number of states of the controller model when a dense approach is used. The controller model can thus be as complex as necessary to generate accurate predictions without increasing the solving time.

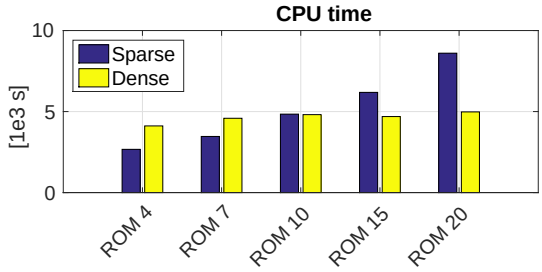

Figure 15: Comparison of the computational demands of the sparse and dense formulation of the control problem.

Acknowledgement

The authors gratefully acknowledge the financial support of the Scientific Grant Agency of the Slovak Republic under the grants 1/0403/15. The authors also acknowledge the financial support by IWT and WTCB in the frame of the IWT-VIS Traject SMART GEOTHERM focusing on integration of thermal energy storage and thermal inertia in geothermal concepts for smart heating and cooling of (medium) large buildings. The modelling work of Arnout Aertgeerts in the frame of the IWT Proeftuin De Schipjes (Integration of sustainable buildings and energy optimization in historical residential clusters) is acknowledged as a good starting point of the models developed in this study.

References

[1] Trent Hilliard, Miroslava Kavgic, and Lukas Swan. Model predictive control for commercial buildings: trends and opportunities. *Advances in Building Energy Research*, 2:172–190, 2015.

[2] Jan Širokỳ, Frauke Oldewurtel, Jiří Cigler, and Samuel Prívara. Experimental analysis of model predictive control for an energy efficient building heating system. *Applied Energy*, 88(9):3079–3087, 2011.

[3] Maarten Sourbron, Clara Verhelst, and Lieve Helsen. Building models for model predictive control of office buildings with concrete core activation. *Journal of Building Performance Simulation*, 6(3):175–198, 2013b.

[4] Samuel Prívara, Jan Široký, Lukáš Ferkl, and Jií Cigler. Model predictive control of a building heating system: The first experience. *Energy and Buildings*, 43(2-3):564–572, February 2011.

[5] Xiwang Li and Jin Wen. Review of building energy modeling for control and operation. *Renewable and Sustainable Energy Reviews*, 37:517–537, 2014.

[6] R. Strand, F. Winkelmann, F. Buhl, J. Huang, R. Liesen, C Pedersen, D. Fisher, R. Taylor, D. Crawley, and L. Lawrie. Enhancing and extending the capabilities of the building heat balance simulation technique for use in energyplus. In *Proceedings of Building Simulation*, volume 2, pages 653–660, Kyoto, Japan, 1999.

[7] S.A. Klein. Trnsys 17, a transient system simulation program. Technical report, Solar Energy Laboratory, University of Wisconsin, Madison, USA, 2010.

[8] M. Wetter, W. Zuo, T. Nouidui, and X. Pang. Modelica buildings library. *Journal of Building Performance Simulation*, 7(4):253–270, 2014.

[9] R. Baetens, R. De Coninck, F. Jorissen, D. Picard, L. Helsen, and D. Saelens. OpenIDEAS - An open framework for integrated district energy simulations. In *Proceedings of Building simulation 2015*, Hyderabad, India, 2015.

[10] Ion Hazyuk, Christian Ghiaus, and David Penhouet. Optimal temperature control of intermittently heated buildings using model predictive control: Part I Building modeling. *Building and Environment*, 51:379 – 387, 2012.

[11] Samuel Privara, Jiri Cigler, Zdenek Vana, Frauke Oldewurtel, Carina Sagerschnig, and Eva Zacekova. Building modeling as a crucial part for building predictive control. *Energy & Buildings*, 56:8–22, January 2013.

[12] Peder Bacher and Henrik Madsen. Identifying suitable models for the heat dynamics of buildings. *Energy and Buildings*, 43(7):1511–1522, 2011.

[13] Glenn Reynders, Jan Diriken, and Dirk Saelens. Quality of grey-box models and identified parameters as function of the accuracy of input and observation signals. *Energy and Buildings*, 82:263–274, 2014.

[14] Kyungtae Yun, Rogelio Luck, Pedro J Mago, and Heejin Cho. Building hourly thermal load prediction using an indexed arx model. *Energy and Buildings*, 54:225–233, 2012.

[15] AE Ruano, EM Crispim, EZE Conceicao, and MMJR Lucio. Prediction of building's temperature using neural networks models. *Energy and Buildings*, 38(6):682–694, 2006.

[16] Dimitrios Gyalistras and Markus Gwerder. Use of weather and occupancy forecasts for optimal building climate control (Opticontrol), two years progress report. Technical report, Terrestrial Systems Ecology ETH Zurich, Zurich, Switzerland, 2009.

[17] B. Lehmann, D. Gyalistras, M. Gwerder, K. Wirth, and S. Carl. Intermediate complexity model for model predictive control of integrated room automation. *Energy and Buildings*, 58(0):250 – 262, 2013.

[18] Damien Picard, Filip Jorissen, and Lieve Helsen. Methodology for obtaining linear state space building energy simulation models. In *Proceedings of the 11th International Modelica Conference*, pages 51–58, Paris, France, 2015.

[19] Tomasz T Gorecki, Faran A Qureshi, and Colin N Jones. OpenBuild: An integrated simulation environment for building control. In *Proceedings of IEEE Conference on Control Applications (CCA)*, pages 1522–1527, Sydney, Australia, 2015.

[20] Aurélie Foucquier, Adrien Brun, Ghjuvan Antone Faggianelli, and Frédéric Suard. Effect of wall merging on a simplified building energy model: accuracy vs number of equations. In *Proceedings of the 13th Conference of International Building Performance Simulation Association*, Chambéry, France, August 2013.

[21] Donghun Kim and James E Braun. Reduced-order building modeling for application to model-based predictive control. In *Proceedings of the 5th National Conference of IBPSA-USA*, volume 5, pages 554–561, Madison, USA, August 2012.

[22] Roel De Coninck. *Grey-Box Based Optimal Control for Thermal Systems in Buildings-Unlocking Energy Efficiency and Flexibility*. PhD, KU Leuven, Leuven, Belgium, 2015.

[23] D. Sturzenegger, D. Gyalistras, V. Semeraro, M. Morari, and R. Smith. BRCM matlab toolbox: Model generation for model predictive building control. In *Proceedings of the American Control Conference*, pages 1063–1069, Portland, USA, June 2014.

[24] M.M. Gouda, Sean Danaher, and C.P. Underwood. Building thermal model reduction using nonlinear constrained optimization. *Building and Environment*, 37(12):1255–1265, 2002.

[25] VSKV Harish and Arun Kumar. Reduced order modeling and parameter identification of a building energy system model through an optimization routine. *Applied Energy*, 162:1010–1023, 2016.

[26] Rick Kramer, Jos Van Schijndel, and Henk Schellen. Simplified thermal and hygric building models: a literature review. *Frontiers of Architectural Research*, 1(4):318–325, 2012.

[27] Xinhua Xu and Shengwei Wang. Optimal simplified thermal models of building envelope based on frequency domain regression using genetic algorithm. *Energy and Buildings*, 39(5):525–536, 2007.

[28] Gilles Fraisse, Christelle Viardot, Olivier Lafabrie, and Gilbert Achard. Development of a simplified and accurate building model based on electrical analogy. *Energy and buildings*, 34(10):1017–1031, 2002.

[29] Damien Picard, Maarten Sourbron, Filip Jorissen, Jiri Cigler, Lukás Ferkl, and Lieve Helsen. Comparison of model predictive control performance using grey-box and white-box controller models. In *Proceedings of the 4th International High Performance Buildings Conference*, pages 1–10, West-Lafayette, Indiana, USA, 2016.

[30] Ruben Baetens. *On externalities of heat pump-based low-energy dwellings at the low-voltage distribution grid*. PhD thesis, Dep. of Civil Engineering, KU Leuven, 2015.

[31] Meteotest. METEONORM version 6.1 - edition 2009. Technical report, Meteotest, 2009.

[32] A. Antoulas. *Approximation of Large-Scale Dynamical Systems*. Society for Industrial and Applied Mathematics, 2005.

[33] Athanasios C Antoulas and Dan C Sorensen. Approximation of large-scale dynamical systems: An overview. *Applied Mathematics and Computer Science*, 11(5):1093–1122, 2001.

[34] D. F. Enns. Model reduction with balanced realizations: An error bound and a frequency weighted generalization. In *Proceedings of the 23rd IEEE Conference on Decision and Control*, pages 127–132, Las Vegas, Nevada, USA, December 1984.

[35] Kenneth Muske and Thomas A. Badgwell. Disturbance modeling for offset-free linear model predictive control. *Journal of Process Control*, 12(5):617 – 632, 2002.

[36] G. Pannocchia and J. B. Rawlings. Disturbance models for offset-free model-predictive control. *AIChE Journal*, 49(2):426–437, February 2003.

[37] G. Frison and J.B. Jorgensen. A fast condensing method for solution of linear-quadratic control problems. In *Proceedings of 52nd IEEE Conference on Decision and Control*, pages 7715–7720, December 2013.

[38] J. Löfberg. YALMIP: A toolbox for modeling and optimization in matlab. In *Proceedings of the CACSD Conference*, Taipei, Taiwan, 2004.

[39] Inc. Gurobi Optimization. Gurobi optimizer reference manual, 2012.